Low-temperature dynamics of water confined in a hydrophobic mesoporous material

PHYSICAL REVIEW E **82**, 020501(R) (2010)

Low-temperature dynamics of water confined in a hydrophobic mesoporous material

Xiang-qiang Chu,[1] Kao-Hsiang Liu,[2] Madhu Sudan Tyagi,[3] Chung-Yuan Mou,[2] and Sow-Hsin Chen[1,*]
[1]*Department of Nuclear Science and Engineering, Massachusetts Institute of Technology, Cambridge, Massachusetts 02139, USA*
[2]*Department of Chemistry, National Taiwan University, 106 Taipei, Taiwan*
[3]*NIST Center for Neutron Research, National Institute for Standards and Technology, Gaithersburg, Maryland 20899, USA*
(Received 7 June 2010; published 26 August 2010)

Quasielastic neutron scattering was used to study the dynamics of three-dimensional confined water in a hydrophobic mesoporous material designated as CMK-1 in the temperature range from 250 to 170 K. We observe a crossover phenomenon at temperature T_L. We find that T_L of water confined in CMK-1 occurs in between previous observations of one-dimensional confined water in materials with different hydrophilicities. This provides the first evidence that besides the obvious surface effect brought about by the hydrophobic confinements, T_L is also dependent on the dimensionality of the geometry of the confinement.

DOI: 10.1103/PhysRevE.82.020501 PACS number(s): 64.70.P−, 61.05.fg, 61.20.Lc

Water in the supercooled temperature range shows many anomalous behaviors, such as an anomalous increase of thermodynamic response functions and an apparent divergent behavior of transport coefficients, toward a singular temperature $T_s=228$ K [1]. With an increasing supercooling, the structural relaxation time of water shows a steeper temperature dependence compare to that of the Arrhenius law. It is known that many glass forming liquids exhibit a fragile behavior (the non-Arrhenius behavior) at moderately supercooled temperatures and then at sufficiently low temperature make a crossover transition to a strong (Arrhenius) liquid [2]. Water is supposed to have a glass transition temperature at $T_g=165$ K [3]. Unfortunately for bulk water, the observation of the fragile to strong dynamic crossover transition, as well as the experimental study of the water behavior around the possible second critical point are impossible due to intervention of the homogeneous nucleation phenomenon. It was predicted [4] that water should also show the transition to a strong liquid in this inaccessible temperature range, around $T_L=228$ K.

Many theoretical simulations and experimental studies showed that the nucleation of water in nanometer size confinement can be strongly suppressed down to about T_g, thus opening an opportunity to study water behavior in this "no man's land" range. A series of quasielastic neutron scattering (QENS) experiments were performed recently on water in porous silica materials MCM-41-S with hydrophilic [5,6] and hydrophobic [7] surfaces, with well calibrated pore size of 10–18 Å, where the freezing process of water was strongly inhibited down to 160 K. It was clearly shown that water in these confinements exhibits a dynamic crossover from fragile to strong liquids at $T_L\approx225$ K [8]. It is also known that water confined in hydrophobic substrate behave differently compared to water confined in hydrophilic substrate [9]. Recent MD simulations predict [10–12] that T_L of water in hydrophobic nanoconfinement can be reduced compared to water in hydrophilic confinement. Furthermore, QENS experiments on water in single-wall carbon nanotubes (SWNT) [13] and double-wall carbon nanotubes (DWNT) [14] showed $T_L=218$ and 190 K, respectively, which is somewhat lower than the result from water confined in hydrophilic MCM-41-S material ($T_L\approx225$ K) [8]. From the above results, the study of water confined in other porous materials with different degrees of hydrophilicity and confined geometry should be of great interest.

In this paper, we study the dynamics of water confined in a hydrophobic mesoporous carbon material CMK-1 by a direct analysis of the incoherent neutron scattering (QENS) spectra using the relaxing cage model (RCM) [15]. Although a recent literature [16] provides evidence that there might be a hydrophobic-hydrophilic transition at some specific temperature, the hydrophilicity of our CMK-1 sample does not change in our measurement range. We analyze the intermediate scattering function (ISF) $F_H(Q,t)$ of hydrogen atoms in the confined water and calculate the so-called *dynamic response function* $\chi_T(Q,t)$ by taking the temperature derivative of $F_H(Q,t)$ numerically [17]. In addition, we compare the crossover temperature of water confined in CMK-1 with the water confined in DWNT [14] and MCM-41 [5] by using a model-independent analysis method [18]. Our result provides the evidence that besides the obvious surface effect brought about by the hydrophobic confinements, the value of the crossover temperature is also dependent on the geometry of the confinement.

The ordered mesoporous carbon CMK-1 [19] was synthesized according to the method of Ryoo *et al.* In brief, it was made by sulfuric acid dehydration of loaded sucrose inside the pores of MCM-48 mesoporous silica (cubic, Ia3d symmetry, consisting of two disconnected interwoven three-dimensional pore systems). Then silica was dissolved by hydrogen fluoride. We use MCM-48-S as template [20], so that compared to regular CMK-1, which has a pore size around 30 Å, our CMK-1–14 has a much smaller pore size of 14 Å. Since CMK-1–14 is composed of amorphous carbon, its surface is uniformly hydrophobic, but not too hydrophobic to be hydrated. Figure 1(a) shows the nitrogen adsorption/desorption isotherm of CMK-1–14. With the Barret-Joyner-Halenda (BJH) analysis, one can obtain the pore volume and the pore diameter as 0.84 cm^3/g and 14 Å, respectively. Thermogravimetry analysis (TGA) of hydrated CMK-1–14 shows a 45% weight loss, which means the hydration level is

*Author to whom correspondence should be addressed. sowhsin@mit.edu

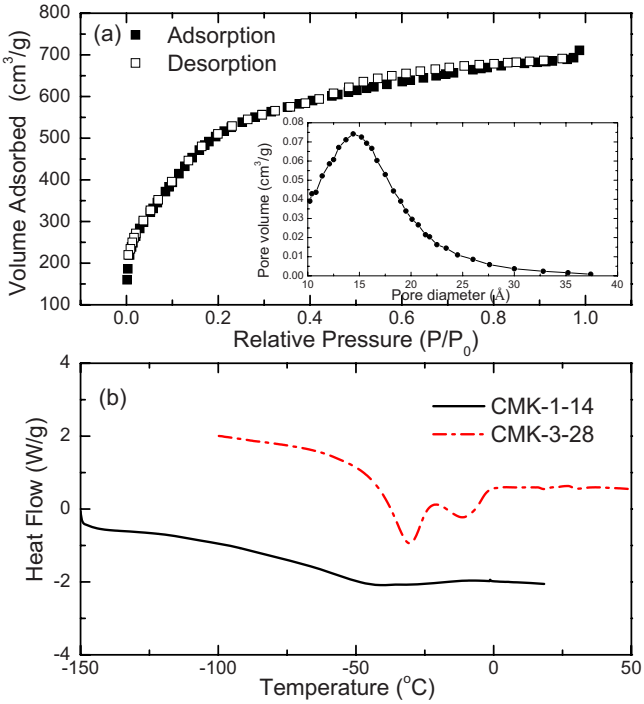

FIG. 1. (Color online) (a) The nitrogen adsorption/desorption isotherm of CMK-1–14 (inset: pore size distribution plot). (b) The differential scanning calorimetry (DSC) results of CMK-1–14 and CMK-3–28, which are taken from 123 to 323 K with the heating rate of 10 K/min.

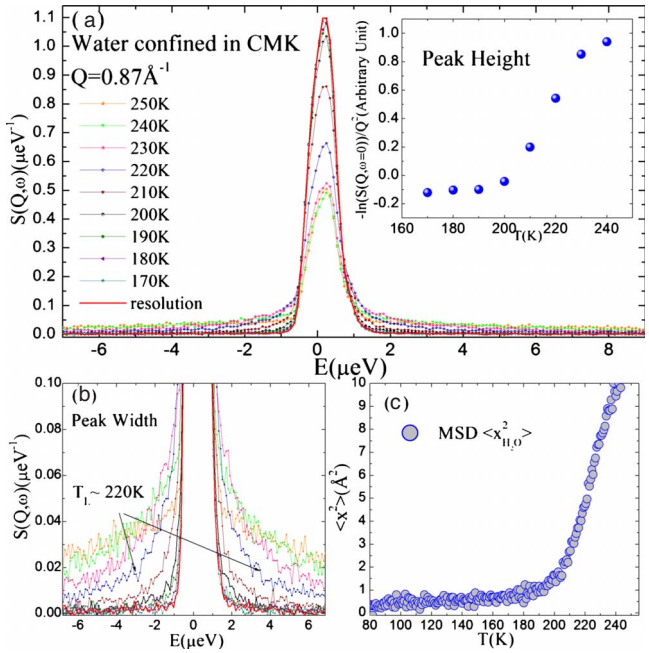

FIG. 2. (Color online) (a) Normalized QENS spectra at a series of temperatures at $Q=0.75$ Å^{-1}. Inset represents the T dependence of the peak heights. We took the logarithm of the peak heights so that it is linearly related to the MSD of the H atoms. (b) The wings of the peaks. (c) MSD of the hydrogen atoms, $\langle x^2_{\mathrm{H_2O}}\rangle$, extracted from the Debye-Waller factor measured by elastic neutron scattering.

at about 98%. Figure 1(b) shows the comparison of the differential scanning calorimetry (DSC) result of CMK-1–14 with another mesoporous carbon material CMK-3–28. The template of CMK-3–28 is SBA-15, instead of MCM-48 for CMK-1–14, so the pore structure is 2D hexagonal and the pore size is 28 Å. One can see that there are two melting peaks in CMK-3–28, which shows the freezing of water in larger pores. Since there is no obvious melting peak down to 150 K, although it is possible that there is a gradual transition to amorphous ice at this temperature range due to the broad range of pore diameter, we believe it is most likely that the water inside CMK-1–14 does not freeze because we can still detect the quasielastic broadening of the liquid state in our QENS experiment.

The QENS experiments were performed using the High-Flux Backscattering Spectrometer (HFBS) at NIST Center for Neutron Research (NCNR) [21]. For the chosen experimental setup, the spectrometer has an energy resolution of 0.8 μeV, full width at half maximum, and a dynamic range of ± 11 μeV, in order to be able to extract the broad range of relaxation times from 1 ps to 10 ns over the temperature range from 250 to 170 K. The QENS measurement gives the self-dynamic structure factor $S_H(Q,\omega)$ of the hydrogen atom in a typical water molecule convolved with the energy resolution function of the instrument. The $S_H(Q,\omega)$ is a Fourier transform of the ISF $F_H(Q,t)$ of the hydrogen atom of the water molecule and can be fitted with the RCM [15]. The RCM describes the translational dynamics of a typical water molecule at supercooled temperature in terms of the product of two functions,

$$F_H(Q,t) = F^S(Q,t)\exp\{-[t/\tau_T(Q)]^{\beta}\}, \quad \tau_T(Q) \cong \tau_0(0.5Q)^{-\gamma}, \tag{1}$$

where the first factor, $F^S(Q,t)$, represents the short-time vibrational dynamics of the water molecule in the cage of its neighbors [15]. The second factor, the α-relaxation term, contains the stretch exponent β, and the Q-dependent translational relaxation time $\tau_T(Q)$, which is a strong function of temperature. The latter quantity is further specified by two phenomenological parameters τ_0 and γ, the prefactor and the exponent controlling the power-law Q-dependence of $\tau_T(Q)$, respectively. The average translational relaxation time, which is a Q-independent quantity we use in this paper, is defined as $\langle\tau_T\rangle = \tau_0\Gamma(1/\beta)/\beta$, where $\Gamma(x)$ is the gamma function. The temperature dependence of the translational relaxation time is calculated from three fitted parameters, τ_0, β, and γ, by analyzing a group of quasielastic peaks at different Q values simultaneously. For this analysis, we chose seven spectra from data taken at HFBS at each temperature [8].

In Figs. 2(a) and 2(b), we plot a set of raw data directly taken from QENS measurements as a function of temperature. Panel (B) shows an enlarged view of the peak wing part in panel (A). It is visible from the inspection of temperature variation of the quasielastic peak height and width that there is some kind of crossover at around 200–220 K. In panel (C) we show the mean-squared atomic displacement (MSD) of the confined water molecule, $\langle x^2_{\mathrm{H_2O}}\rangle$, in the observational time interval about 2 ns (corresponding to the

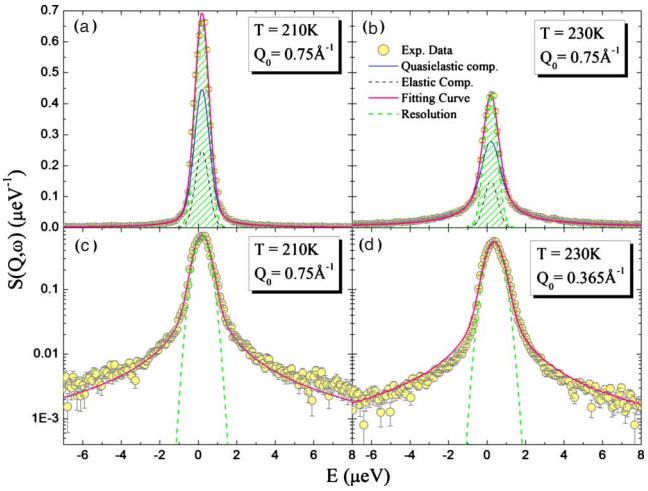

FIG. 3. (Color online) RCM analysis of QENS spectra taken at two typical temperatures T=210 K [(a), (c)], 230 K [(b), (d)] at Q=0.75 Å^{-1} and 0.365 Å^{-1}. Panels (a) and (b) are plotted in linear scale and panels (c) and (d) are plotted in logarithm scale. The red (dark gray) solid line represents the fitted curve using the RCM model. The green (gray) dashed line is the Q-dependent instrumental resolution function. The dotted line represents the elastic component in the fitting. Error bars throughout the paper represent standard deviation.

energy resolution of 0.8 μeV). One can observe a sudden change of the slope at around 200 K. This temperature is about 25 K lower than the one we recently observed from the MSD of Lysozyme hydration water [22] and the one we obtained from the MSD of water confined in MCM-41-S [23]. On the other hand, it is 10 K higher than what we observed in the MSD of water confined in DWNT [14].

Figure 3 illustrates the process of the RCM analysis. It is shown that the RCM analysis agrees with the measured QENS data satisfactorily. The comparison was made of the data taken from temperatures just above and below the crossover temperature T_L. As the temperature decreases, the dynamics of water slows down, and the bulk of the fluctuations are so slow that they could be seen as immobile by the QENS spectrometers. We thus use a term of elastic component [8] in our analysis to keep the RCM still valid and the elastic contribution is shown to be increasing as the temperature decreases.

By analyzing the QENS spectra using RCM [15], we are able to calculate the ISF $F_H(Q,t)$ of the typical hydrogen atom in water molecules. From the ISF we then construct the *dynamic response function* $\chi_T(Q,t)$ [17]. Analogously, in order to describe the dynamic response of a system to an external perturbation ΔT, we can take the temperature derivative of the time-dependent state functions, such as the single-particle density correlation function $F_H(Q,t)$. We thus define $\chi_T(Q,t)$ as

$$\chi_T(Q,t) = -\left(\frac{\partial F_S(Q,t)}{\partial T}\right)_P. \tag{2}$$

The $\chi_T(Q,t)$ generally shows a single peak when plotted as a function of time at constant Q. The peak position occurs at around the Q-dependent translational relaxation time $\tau(Q,T)$ [8] containing in the exponent of the ISF $F_H(Q,t)$. The height of the peak is proportional to some sort of dynamic correlation length [17,18,24,25].

In Fig. 4(a) we show the ISF calculated by Eq. (1) from the fitting parameters β, τ_0, and γ at several temperatures of the water confined in CMK-1 as a function of time. Figure

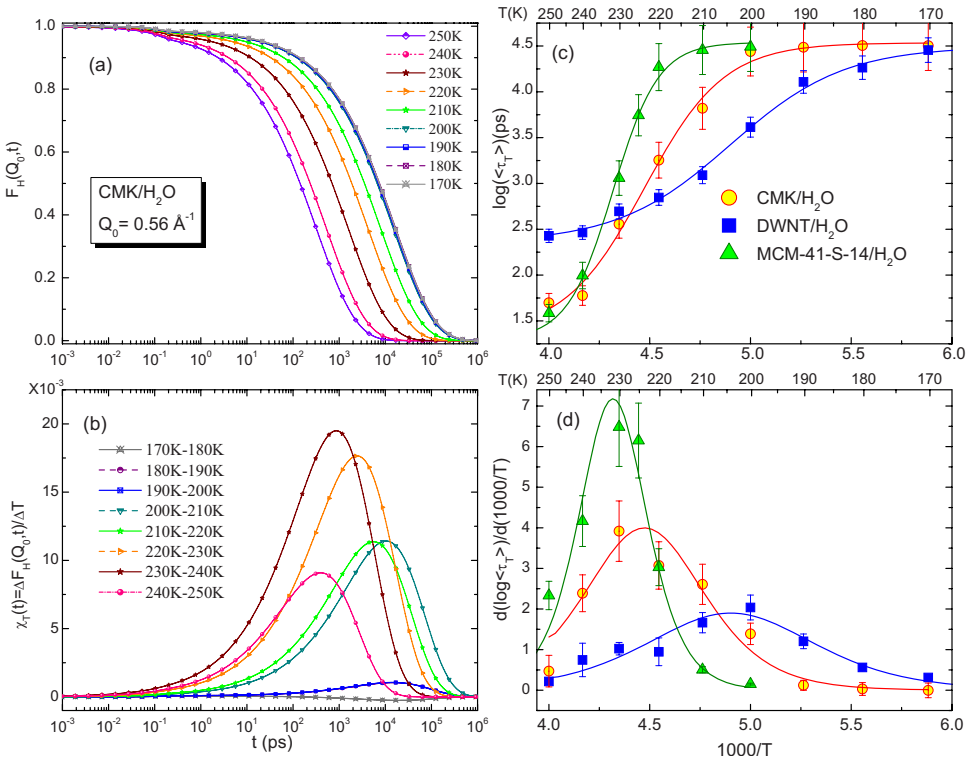

FIG. 4. (Color online) (a) The self-intermediate scattering functions (ISF) of hydrogen atoms in water confined in CMK, extracted from analysis of QENS data. We show here the specific case at Q =0.56 Å^{-1} for nine temperatures, ranging from 250 to 170 K. (b) Dynamic response function $\chi_T(Q,t)$, calculated from the ISF shown in panel (a). (c) Comparison of the extracted average translational relaxation time $\langle\tau_T\rangle$ of water confined in CMK-1 with those of water in MCM-41-S and DWNT. (d) Derivative of the Arrhenius plot of the α-relaxation time, $d\log(\langle\tau_T\rangle)/d(1/T)$, for the three cases in panel (c). The peak position in panel (d) is a suitable indicator of the crossover temperature T_L in each case.

4(b) shows a series of dynamic response functions $\chi_T(Q,t)$ calculated from the ISF shown in (A). The peak height of $\chi_T(Q,t)$, $\chi_T^*(Q)$, grows as T is lowered and reaches a maximum at $T_L=230\pm5$ K, but this growth is interrupted when the dynamic crossover sets in. The only parameter in $F_H(Q,t)$ that has to be differentiated with respect to T is $\tau_T(Q,T)$, since β remains almost constant and close to 0.5 ± 0.1 as T is lowered [7,18]. $\chi_T^*(Q)$ is therefore directly proportional to the change of slope of the Arrhenius plot of $\tau_T(Q,T)$ [Fig. 4(c)]. Therefore, this change of slope in the Arrhenius plot of $\tau_T(Q,T)$ is in our opinion the most unbiased way of defining the crossover temperature.

Thus here we use the model-independent determination of the crossover temperature to determine T_L. It is by taking the slope of the translational relaxation time $\langle\tau_T\rangle$ in its Arrhenius plot, i.e., $d\log\langle\tau_T\rangle/d(1/T)$. The peak position in the $d\log\langle\tau_T\rangle/d(1/T)$ vs $1/T$ plot represents the temperature where the largest slope in the Arrhenius plot occurs and is a suitable indicator of the crossover temperature T_L. The T_L determined by this method is usually 10–20 K higher than the one determined by the traditional method (fitting the Arrhenius plot with the Arrhenius law at low temperatures and with the Vogel-Fulcher-Tammann (VFT) law at high temperatures respectively) [5,6,8,14]. In Figs. 4(c) and 4(d) we compare the $\log\langle\tau_T\rangle$ vs $1/T$ plots of water confined in three different materials, CMK-1, DWNT [14] and MCM-41-S [5] and can find from the peak position in panel (D) that the maximum slope in the Arrhenius plot of $\langle\tau_T\rangle$ for CMK-1 appears at a temperature about $T_L=225\pm5$ K. This temperature agrees within the error bar with the temperature $T_L=230\pm5$ K shown in panels (A) and (B), at which the maximum in the peak height of the calculated dynamic response function $\chi_T(Q,t)$ appears. In addition, we can clearly see that the crossover temperature T_L of the CMK-1 is slightly lower than that of the MCM-41-S (235 ± 5 K), but higher than that of the DWNT (205 ± 5 K).

In conclusion, we determine the crossover temperature by the model-independent analysis of the average translational relaxation time $\langle\tau_T\rangle$ by computing $d\log\langle\tau_T\rangle/d(1/T)$ as a function of T. The crossover temperature T_L is 225 ± 5 K for water confined in CMK-1 hydrophobic substrate. It decreases by ΔT_L of about 10 K as compare to water confined in hydrophilic substrate MCM-41-S. While for DWNT case, ΔT_L is about 30 K instead. From this result, CMK-1 is seen to be not a completely hydrophobic material and its hydrophilicity is in-between MCM-41-S and DWNT cases. The value of ΔT_L may also be dependent on the geometry of the hydrophobic confinement [three-dimensional (3D) in the case of CMK-1 as compare to one-dimensional (1D) in the case of DWNT]. The peak height of the dynamic response function $\chi_T(Q,t)$ as a function of temperature is another way of determining the crossover temperature. However, this method suffers from the inaccuracy due to the large temperature interval between different measurement points and thus has big error bars. Our results show that the dynamics of water under temperatures below 170 K is so slow that it runs to the limit of the instrumental resolution. However, our previous experiments [6,22] indicate that the relaxation time of water molecules are shorter under pressure. Thus studying the pressure effects on water dynamics under hydrophobic confinement should be another interesting topic to be investigated in the future.

Research at MIT was supported by Department of Energy Grant No. DE-FG02-90ER45429; at NTU, it was supported by Taiwan National Science Council Grants No. NSC95-2120-M-002-009 and No. NSC96-2739-M-213-001. This work utilized facilities supported in part by the National Science Foundation under Agreement No. DMR-0086210. We appreciate technical supports during experiments from A. Faraone and T. Jenkins of NIST Center for Neutron Research.

[1] R. J. Speedy and C. A. Angell, J. Chem. Phys. **65**, 851 (1976).
[2] P. Taborek, R. N. Kleiman, and D. J. Bishop, Phys. Rev. B **34**, 1835 (1986).
[3] V. Velikov, S. Borick, and C. A. Angell, Science **294**, 2335 (2001).
[4] K. Ito, C. T. Moynihan, and C. A. Angell, Nature (London) **398**, 492 (1999).
[5] A. Faraone, L. Liu, C. Y. Mou, C. W. Yen, and S. H. Chen, J. Chem. Phys. **121**, 10843 (2004).
[6] L. Liu, S. H. Chen, A. Faraone, C. W. Yen, and C. Y. Mou, Phys. Rev. Lett. **95**, 117802 (2005).
[7] A. Faraone, K. H. Liu, C. Y. Mou, Y. Zhang, and S. H. Chen, J. Chem. Phys. **130**, 134512 (2009).
[8] L. Liu *et al.*, J. Phys.: Condens. Matter **18**, S2261 (2006).
[9] D. Chandler, Nature (London) **437**, 640 (2005).
[10] P. Kumar, S. V. Buldyrev, F. W. Starr, N. Giovambattista, and H. E. Stanley, Phys. Rev. E **72**, 051503 (2005).
[11] P. Kumar, S. H. Han, and H. E. Stanley, J. Phys.: Condens. Matter **21**, 504108 (2009).
[12] G. Franzese, and F. de los Santos, J. Phys.: Condens. Matter **21**, 504107 (2009).
[13] E. Mamontov *et al.*, J. Chem. Phys. **124**, 194703 (2006).
[14] X. Q. Chu, A. I. Kolesnikov, A. P. Moravsky, V. Garcia-Sakai, and S. H. Chen, Phys. Rev. E **76**, 021505 (2007).
[15] S. H. Chen, C. Liao, F. Sciortino, P. Gallo, and P. Tartaglia, Phys. Rev. E **59**, 6708 (1999).
[16] H. J. Wang, X. K. Xi, A. Kleinhammes, and Y. Wu, Science **322**, 80 (2008).
[17] L. Berthier *et al.*, Science **310**, 1797 (2005).
[18] Y. Zhang *et al.*, Phys. Rev. E **79**, 040201 (2009).
[19] R. Ryoo, S. H. Joo, and S. Jun, J. Phys. Chem. B **103**, 7743 (1999).
[20] C. C. Chen, Master Thesis, National Taiwan University, 2008.
[21] A. Meyer, R. M. Dimeo, P. M. Gehring, and D. A. Neumann, Rev. Sci. Instrum. **74**, 2759 (2003).
[22] X. Q. Chu *et al.*, J. Phys. Chem. B **113**, 5001 (2009).
[23] L. Liu *et al.* (unpublished data in 2005).
[24] S. H. Chen *et al.*, Z. Phys. Chemie-Int. J. Res. Phys. Chem. Chem. Phys. **224**, 109 (2010).
[25] L. Berthier *et al.*, J. Chem. Phys. **126**, 184503 (2007).